The sucrose non-fermenting-1 kinase Snf1 is involved in fludioxonil resistance via interacting with the high osmolarity glycerol MAPK kinase Hog1 in *Fusarium*

Jing Wang[1,2], Ziyue Wen[1], Yun Chen[1] and Zhonghua Ma[1*]

Abstract

Fusarium head blight (FHB) caused by *Fusarium graminearum* complex is a worldwide devastating disease of wheat, barley, maize, and other cereals. In the field, application of fungicides is one of the main strategies for management of FHB. With the long-time usage of fungicides, resistant pathogen populations have become a new challenge for disease management. Application of new pesticide is necessary for sustainable control of this disease. The phenylpyrrole fungicide fludioxonil has been registered recently for management of FHB. However, the resistance mechanisms of *F. graminearum* to this compound are largely unknown. Here we isolated a biocontrol bacterium *Burkholderia pyrrocina* W1, which produced the antifungal compound pyrrolnitrin and showed greatly antagonistic activity towards FHB. Spontaneous mutants of pyrrolnitrin-resistant *F. graminearum* were induced and re-sequenced. Single base mutations were identified in the genes encoding the osmoregulation MAP kinase Hog1 and the AMP dependent kinase Snf1 in pyrrolnitrin-resistant mutants. Snf1 was further confirmed to interact with Hog1 and involved in the response of this fungus to pyrrolnitrin and its derivate, the fungicide fludioxonil. This study reveals that the Snf1 interacts with Hog1 to regulate fludioxonil resistance in a pathogenic fungus.

Keywords *Fusarium graminearum*, Pyrrolnitrin, Fludioxonil, Fungicide resistance, HOG pathway, Snf1 kinase

Background

Pathogens and pests cause about 17 to 30% crop losses for wheat, rice, maize, potato, and soybean in the field worldwide (Van Bergeijk et al. 2020). *Fusarium graminearum*, one of the top ten fungal phytopathogens, causes Fusarium head blight (FHB) on cereal crops of wheat, barley, and maize, resulting in great yield loss and mycotoxin concerns in the epidemic year (Starkey et al. 2007; Dean et al. 2012). To date, benzimidazoles, SBIs (Sterol Biosynthesis Inhibitors), and the novel cyanoacrylate phenamacril and their mixtures have become the most widely used fungicides for management of FHB in China (Chen et al. 2011; Sun et al. 2014). However, fungicide-resistant *F. graminearum* strains have been detected in several regions, and these resistant strains may produce more mycotoxin than the sensitive ones (Tang et al. 2018; Chen et al. 2019). Thus, developing alternative strategies for management of FHB is of great importance for FHB control.

Microbial biocontrol has gained much attention recently following the advance of microbiology and microbiome (Wargo and Hogan 2006; Raymaekers et al.

*Correspondence:
Zhonghua Ma
zhma@zju.edu.cn
[1] State Key Laboratory of Rice Biology, and Key Laboratory of Molecular Biology of Crop Pathogens and Insects, Institute of Biotechnology, Zhejiang University, Hangzhou 310058, China
[2] College of Plant Protection, Southwest University, Chongqing 400715, China

Wang *et al. Phytopathology Research*   (2023) 5:52

Page 2 of 13

2020). Screening of bio-control agents (BCAs) that produce highly active compounds have been used extensively (Xu et al. 2011; Raymaekers et al. 2020). The active compound pyrrolnitrin was firstly identified as the secondary metabolite of *Pseudomonas pyrrocinia* and showed strong antifungal activity against multiple plant and animal pathogens, including *Rhizoctonia solani*, *Alternaria* sp., *Fusarium* sp., *Verticillium dahliae*, and *Trielaviopsis basicola* (Arima et al. 1965). Although the antifungal activity of pyrrolnitrin is stable for 30 days in the soil, it is vulnerable to light decomposition (Howell and Stipanovic 1979). Later, fludioxonil and fenpiclonil were developed as analogs of pyrrolnitrin by CibaGeigy AG (now Syngenta AG) in 1980s and were introduced into the market for seed treatment and foliar use (Kilani and Fillinger 2016). With a strong inhibitory activity against the growth of *F. graminearum* in laboratory and field, fludioxonil was registered for FHB control in China recently (http://www.icama.org.cn/).

It was reported that exposure to the phenylpyrrole compounds, including pyrrolnitrin, fludioxonil, and fenpiclonil, caused amino acids and lipids accumulation and the osmotic signaling activation in the target fungi, which requires the presence of a group III hybrid histidine kinase (HHK) (Motoyama et al. 2005; Lew 2010; Kilani and Fillinger 2016). The compounds triggered the conversion of HHK to a phosphatase, which dephosphorylated the histidine phosphotransfer protein Ypd1 to constitutively activate HOG signaling (Lawry et al. 2017). Later, Brandhorst and the colleagues studied the action of fludioxonil on the group III HHK Drk1 (dimorphism-regulating kinase 1) in *Saccharomyces cerevisae*, where they demonstrated that this chemical interfered with TPI (triosephosphate isomerase), leading to the release of methylglyoxal (MG), an activator of group III HHK and HOG pathway (Brandhorst et al. 2019). However, the direct targets of these compounds remain uncharacterized yet. In addition, although with high efficiency and stability, a few fludioxonil resistant strains were identified recently (Li and Xiao 2008; Wang et al 2021; Wen et al. 2022). Thus, it is necessary to investigate the underlined resistant mechanisms and the regulatory network of fludioxonil-responsible osmotic signal pathway in pathogenic fungi.

Snf1 (Sucrose non-fermenting-1) kinase was initially identified in *S. cerevisae* as the orthologue of mammalian AMP-activated protein kinase (AMPK), which balances the catabolism and photosynthesis through maintaining the rate of ATP consumption and energy homeostasis (Mitchelhill et al. 1994; Hardie 2007). In the budding yeast, Piao et al (2012) found that Hog1 is rapidly activated by both glucose starvation and glucose stimulation, which is independent of the well-characterized response to osmotic stress but is controlled by Snf1. Elimination of either Hog1 or Snf1 slows glucose-induced translocation of lipid phosphatase Sac1 from the Golgi to the endoplasmic reticulum (ER), indicating that a novel cross-talk between the HOG pathway and Snf1/AMPK is required for the metabolic control of lipid signaling at Golgi. To date, it remains elusive whether there is a cross-talk between the SNF1 and the HOG MAPK pathways, or whether the SNF1 pathway participates in fungicide response in filamentous fungi.

In this study, we identified a biocontrol agent *Burkholderia pyrrocina* strain W1 with a greatly antagonistic activity against *F. graminearum* in both laboratory and field tests. Through fermentation, purification, and HPLC-MS identification, we determined that the major antifungal compound of this biocontrol agent is pyrrolnitrin. In addition, spontaneous resistant mutants were obtained from the PDA plates supplemented with pyrrolnitrin. Genomic resequencing of these mutants identified multiple single base mutations in several encoding genes, including the genes encoding osmoregulation MAP kinase Hog1 and AMP kinase Snf1. Further, we found that Snf1 interacted with Hog1 and was involved in the fludioxonil response in this fungus. Current work revealed a new cross-talk between Snf1 and the Hog1 pathway in regulating fungal response to fludioxonil, which would be informative for management of fludioxonil resistance.

Results

Burkholderia pyrrocina W1 shows strong inhibitory activity towards FHB

A total of 6070 bacterial strains isolated from 30 rhizosphere samples of wheat were confronted with *F. graminearum*. Among them, four strains showed great antagonistic activity towards the pathogen, which produced a radius of inhibition zone > 15 mm when they were co-cultivated with *F. graminearum* (Fig. 1a). To identify these strains, the 16S rRNA fragments were amplified and sequenced. BLAST assays of these sequences in the National Center for Biotechonology and Information (NCBI) database (https://blast.ncbi.nlm.nih.gov/Blast.cgi) showed that all four strains belong to the genus of *Burkhholderia*, thus they were named as *Burkhholderia* W1 to W4. Since the colony phenotypes of these four *Burkhholderia* strains were similar and they showed similar inhibitory activity on *F. graminearum* (Fig. 1a), we chose W1 for further study. This strain was further identified as *Burkholderia pyrrocina* based on its 16S rRNA sequence, and termed BpW1 hereafter. When co-cultivated with BpW1, *F. graminearum* showed severe morphological and developmental defects. Mycelial compartments of the wild type strain PH-1 that was co-cultivated with
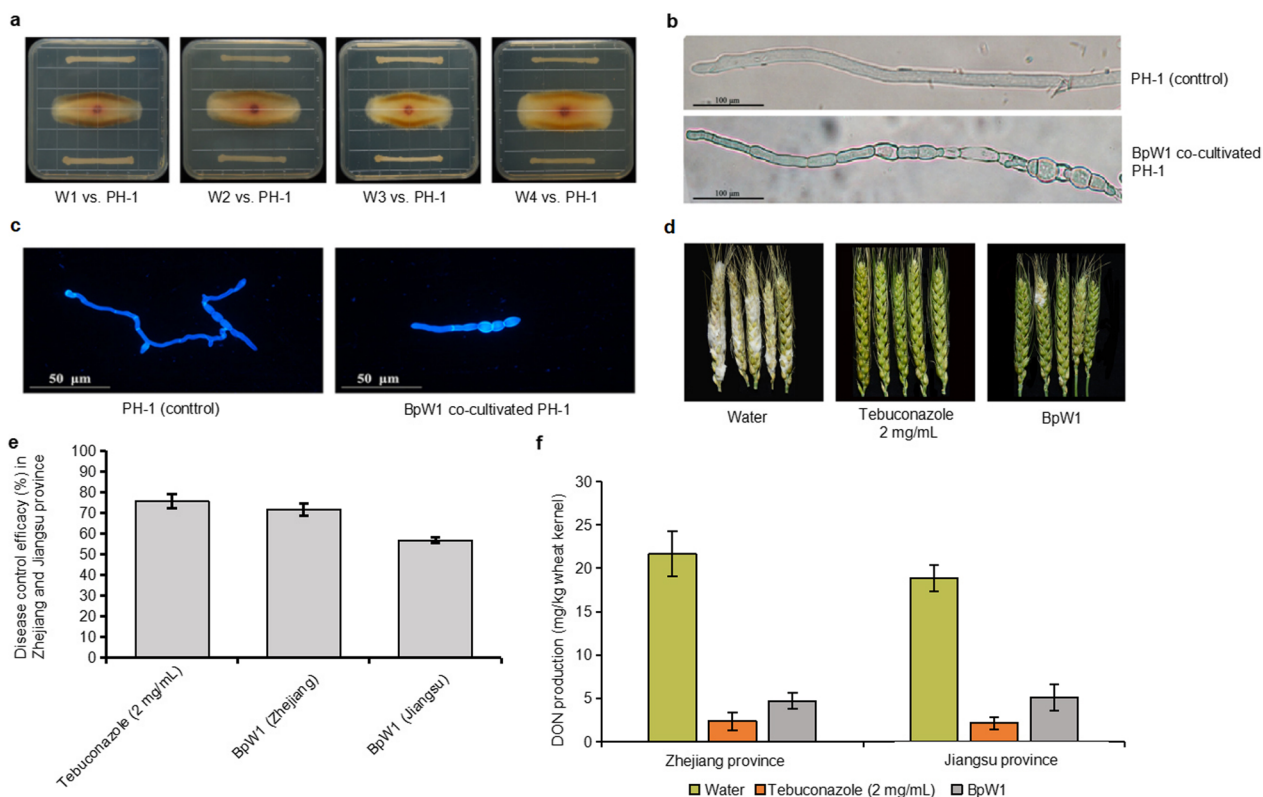
Wang *et al. Phytopathology Research*   (2023) 5:52

Page 3 of 13

Fig. 1 *Burkholderia pyrrocina* W1 exhibits strong inhibitory activity towards FHB caused by *F. graminearum*. **a** *Burkholderia* W1–W4 displayed comparable antagonistic activity towards mycelial growth of *F. graminearum*. **b** *Burkholderia pyrrocina* W1 (BpW1) caused swelling and abnormal hypha of *F. graminearum*. **c** BpW1 inhibited the spore germination of *F. graminearum*. **d** BpW1 displayed high activity against FHB in detached wheat head. **e** BpW1 was effective against FHB in field. **g** BpW1 inhibited DON production in the field experiments. A concentration of 2 mg/mL tebuconazole and water were used as fungicide and negative controls in Fig. 1d–f, respectively

BpW1 became swelling and vacuolization, leading to the tortuous and malformed hyphae (Fig. 1b). Meanwhile, BpW1 showed high activity against PH-1 spore germination (Fig. 1c). Moreover, BpW1 also showed high inhibitory activity to these carbendazim-resistant *F. graminearum* strains identified previously (Additional file 1: Figure S1).

To determine the inhibitory activity of BpW1 against FHB *in planta*, biocontrol experiments were conducted in both the growth chamber and the field using the fungicide tebuconazole and water served as positive and negative controls, respectively. BpW1 suppressed infection of *F. graminearum* on wheat heads significantly in growth chamber assays (Fig. 1d). Consistent with its highly antifungal activity in growth chamber, BpW1 showed a biocontrol efficacy of 60.78%–71.56% against FHB in field, which is comparable to the fungicide tebuconazole (Fig. 1e). In addition, BpW1 reduced deoxynivalenol (DON) production significantly in field trials (Fig. 1f).

Pyrrolnitrin is an antagonistic compound produced by BpW1

Previous studies showed that some *Burkhholderia* strains have been used as biological control agents because they produce antifungal metabolites, including cepacin, cepaciamide, xylocandins, pseudanes, phenylpyrroles, and phenazine (Parker et al. 1984; Lee et al.1994; Cartwright et al. 1995; Jiao et al. 1996; Moon et al. 1996). To determine the inhibitory mechanisms of BpW1 towards FHB, the secondary metabolites of this strain were analyzed. Firstly, we tested the antagonistic activity of the cell-free supernatant (CFS) of BpW1 to determine whether the antifungal compounds exist in the cell-free culture supernatant or not. Expectedly, the BpW1 CFS showed a high inhibitory activity against the mycelial growth of *F. graminearum* (Fig. 2a). Subsequently, active compounds in the supernatant of BpW1 were further extracted with acetonitrile and dissolved in methanol. The compounds were subjected to ultra performance liquid chromatography (UPLC) coupled with tandem
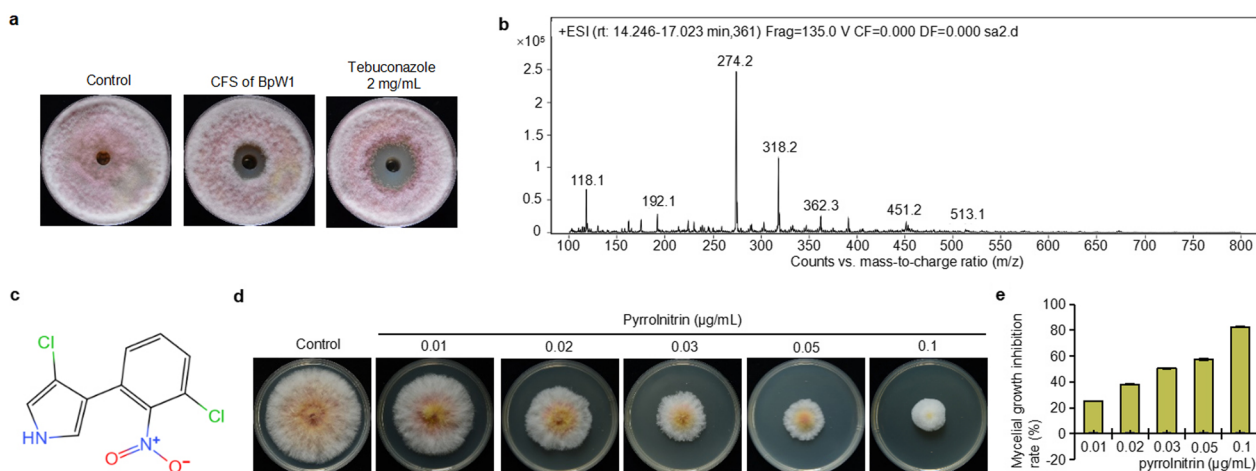
Wang *et al. Phytopathology Research*   (2023) 5:52

Page 4 of 13

Fig. 2 Pyrrolnitrin is an antagonistic compound produced by BpW1. **a** The cell free supernatant (CFS) of BpW1 showed strong inhibitory activity towards the spore germination and vegetative growth of *F. graminearum*. The fungicide tebuconazole and water were used as positive and negative controls, respectively. **b** The MS/MS diagram of the peak at 15.5 min in UPLC analysis. **c** The structural formula of pyrrolnitrin. **d** Antifungal activities of pyrrolnitrin against mycelial growth of *F. graminearum* on PDA plates. **e** Inhibition rate calculated according to the sensitivity test

mass spectrometry (MS/MS) analysis. A distinct peak at 15.5 min was detected in the total ion chromatogram (TIC) (Additional file 1: Figure S2a). The retention time and mass-to-charge ratio character of this peak were same as the standard substance of pyrrolnitrin (Fig. 2b and Additional file 1: Figure S2b, c), indicating that this compound is pyrrolnitrin (Fig. 2c). Antifungal activity assay showed that the commercialized pyrrolnitrin displayed a great inhibitory effect against vegetative growth of *F. graminearum*, with the EC_{50} value of 0.041 μg/mL (Fig. 2d, e).

Protein kinase Snf1 is involved in fludioxonil resistance in *F. graminearum*

To investigate the antifungal mechanism of pyrrolnitrin to *F. graminearum*, we tried to induce resistance mutations of the pathogen on the pyrrolnitrin-containing PDA plates, resulting in six pyrrolnitrin resistant strains that were named as PRS1-6. Since the morphologies and pyrrolnitrin-sensitivities of the six strains were similar, a representative PRS-1 was examined (Fig. 3a, b and Additional file 1: Figure S3). To identify the mutation sites in these six resistant mutants, their genomic DNAs were re-sequenced and compared with the parent PH-1 strain (NRRL31084). Resequencing of the pyrrolnitrin-resistant mutants identified base mutations in coding regions of several genes (Additional file 2: Table S1). In addition to the mutations in the HOG MAPK pathway, including histidine kinases FgOS1, FgOS4, and FgOS5, mutations were also discovered in two transcription factors (FgAreA and FgStuA) and the protein kinase FgSnf1 (coded by gene locus FGSG_09897). These mutations resulted in amino

acid mutations or frame shift but not premature termination. For instance, the deletion of 668th thymine (T) on the encoding region of FgSnf1 caused the shift of opening reading frame from the 233th codon cysteine (Cys) (Additional file 2: Table S1). Previous works have demonstrated that deletion or mutation of histidine kinase OS1, OS4, or OS5 resulted in decreased sensitivity to fludioxonil in *F. graminearum* and other fungi (Zheng et al. 2012; Zhou et al. 2020; Wen et al. 2022). Thus, we were interested in testing the sensitivity of FgHog1, FgSnf1, FgAreA, and FgStuA deficient mutants to fludioxonil or pyrrolnitrin. Compared with the wild type strain PH-1, the FgSnf1 deletion mutant Δ*FgSNF1* exhibited resistance to fludioxonil at 0.01 μg/mL, but not at higher concentrations, and the sensitivity of Δ*FgSNF1* to pyrrolnitrin was changed similarly. Moreover, the FgHog1 deletion mutant (Δ*FgHOG1*) and the pyrrolnitrin-resistant strain PRNJB3-2 isolated from the field were highly resistant to fludioxonil and pyrrolnitrin (Fig. 4a, b, and Additional file 1: Figure S4a, b); whereas, the deletion mutants of FgAreA and FgStuA exhibited an increased sensitivity to pyrrolnitrin (Additional file 1: Figure S4c, d), but the exact mechanisms remain uncharacterized.

Previous study showed that the cellular glycerol accumulation was increased in fungal cells upon fludioxonil treatment (Wen et al. 2022). But it is unknown whether FgSnf1 is related to glycerol accumulation or not. Therefore, the glycerol accumulations were tested in PH-1 and Δ*FgSNF1* with or without fludioxonil treatment. As shown in Fig. 4c, the glycerol level was significantly improved in the wild type PH-1 strain under fludioxonil treatment, while the glycerol level in Δ*FgSNF1* without
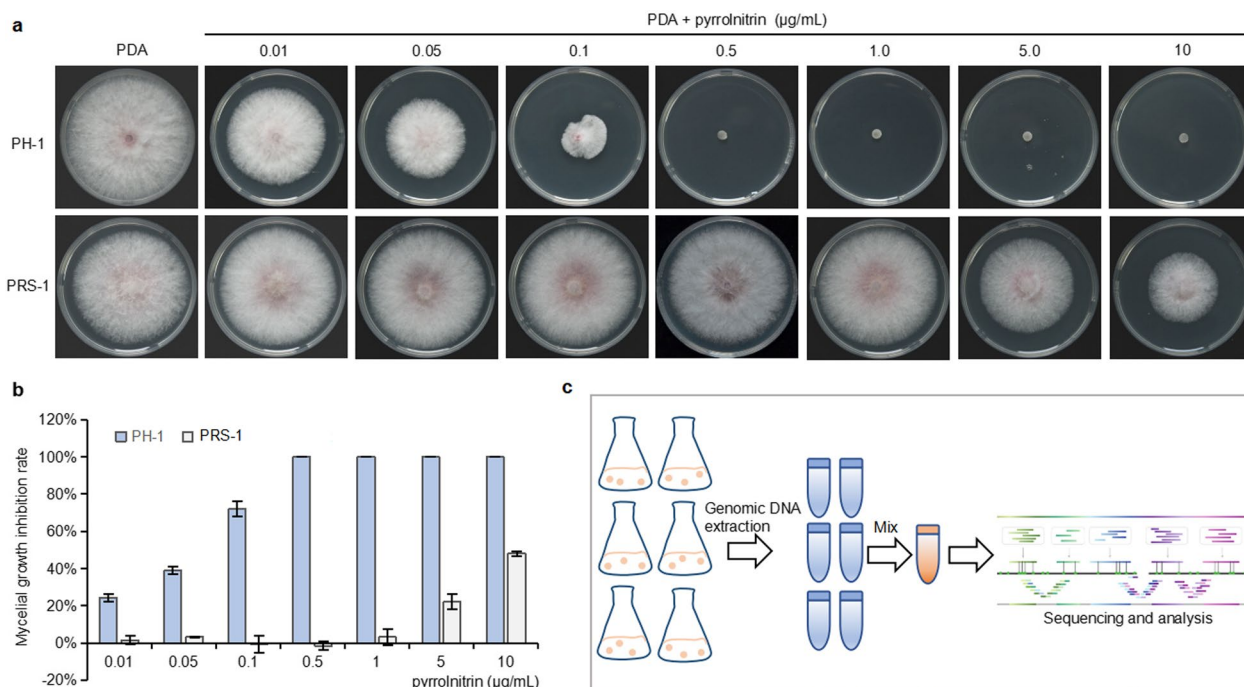
Fig. 3 Sensitivity of laboratory induced pyrrolnitrin-resistant strain PRS-1 to pyrrolnitrin. **a** Sensitivity of the wild-type PH-1 and the pyrrolnitrin-resistant strain PRS-1 to pyrrolnitrin. **b** Inhibition rate calculated according to the sensitivity test. **c** The schematic diagram for re-sequencing pyrrolnitrin-resistant strains

fludioxonil treatment was comparable to that in the fludioxonil-treated PH-1. In addition, fludioxonil stimulation did not cause a further change of glycerol accumulation in ΔFgSNF1. Taken together, these results indicate that the Snf1 kinase is associated with fludioxonil sensitivity in *F. graminearum*.

Snf1 represses the activation of HOG signaling pathway
The activation of HOG MAPK pathway is widely accepted as a fungal response to fludioxonil (Kojima et al. 2006). Currently, the association of Snf1 with the HOG pathway in regulating fungicide sensitivity is unknown. To answer this question, we examined the phosphorylation of Hog1 under the stimulus of fludioxonil. In the wild type PH-1, the phosphorylation of Hog1 was enhanced significantly upon fludioxonil treatment, which is consistent with the previous finding (Wen et al. 2022); whereas, the situation is much different in *Snf1* mutant. The phosphorylation level of FgHog1 in the FgSnf1 deletion mutant was comparable to that of fludioxonil treated PH-1, but fludioxonil treatment led to a higher phosphorylation level of FgHog1 in the mutant (Fig. 5a, b). Since the activation of Hog1 is associated with its nuclear import, we observed the sub-cellular localization of C-terminal GFP fused FgHog1 (termed as FgHog1-GFP). Consistent with the phosphorylation levels, fludioxonil treatment promoted the nuclear import of FgHog1-GFP in the wild-type

PH-1, but its nuclear localization is constantly prominent in FgSnf1 deletion mutant even without fludioxonil treatment (Fig. 5c). These results indicate that the FgSnf1 acts as a repressor for the fludioxonil-stimulated activation of FgHog1.

To figure out whether FgSnf1 affects the activation FgHog1 directly, we tested the interactions between FgSnf1 and FgHog1 in Y2H (yeast two hybrid) and Co-IP (co-immunoprecipitation) assays. As shown in Fig. 5d, FgSnf1 was able to interact with FgHog1 directly in Y2H assays (Fig. 5d). In addition, using the specific antibody against Hog1, the FgHog1 was detected in the precipitates of FgSnf1-Flag in PH-1 (Fig. 5e), which further confirmed the interaction between FgSnf1 and FgHog1. Taken together, these data indicate that FgSnf1 interacts with Hog1 and FgSnf1 represses the phosphorylation of Hog1 in *F. graminearum*.

Snf1 is required for full virulence and DON biosynthesis of *F. graminearum*
The virulence of each strain was evaluated by point-inoculating with fresh mycelia on flowering wheat head. Fifteen days after inoculation, the wild-type PH-1 caused typical scab symptom on the wheat head, while wheat heads of the control (water treatment) were green and healthy. Notably, ΔFgSNF1 and ΔFgHOG1 showed decreased virulence on wheat head (Fig. 6a). In addition,
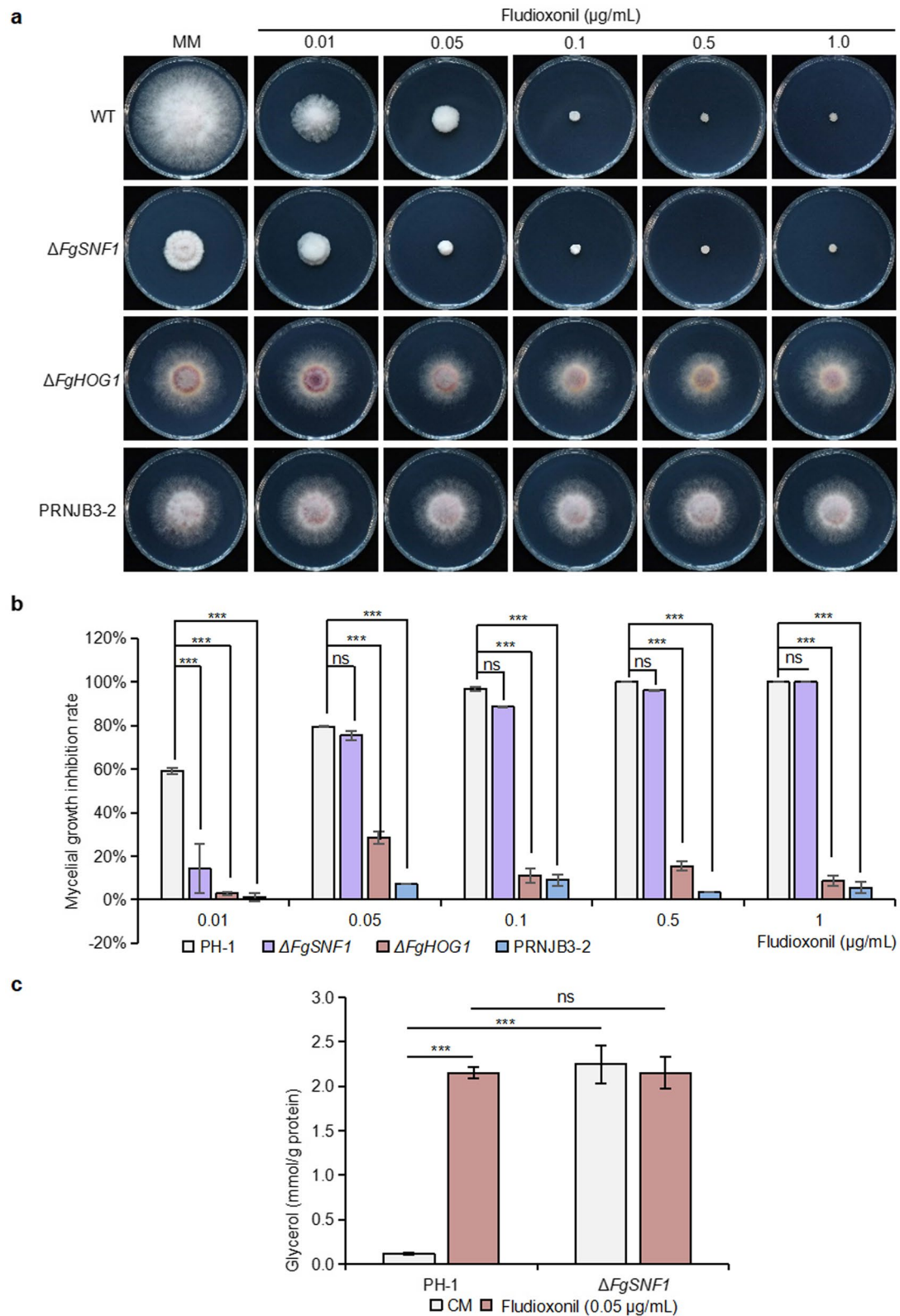
Fig. 4 Protein kinases FgSnf1 and FgHog1 are associated with fludioxonil resistance in *F. graminearum*. **a** Sensitivity of PH-1, Δ*FgSNF1*, Δ*FgHOG1*, and the fludioxonil-resistant PRNJB3-2 strains to fludioxonil at different concentrations. **b** Mycelial growth inhibition rate quantified from a. **c** Glycerol accumulation in PH-1 and Δ*FgSNF1* treated with or without fludioxonil. *** indicates significantly different at $P = 0.001$. ns refers no significant difference
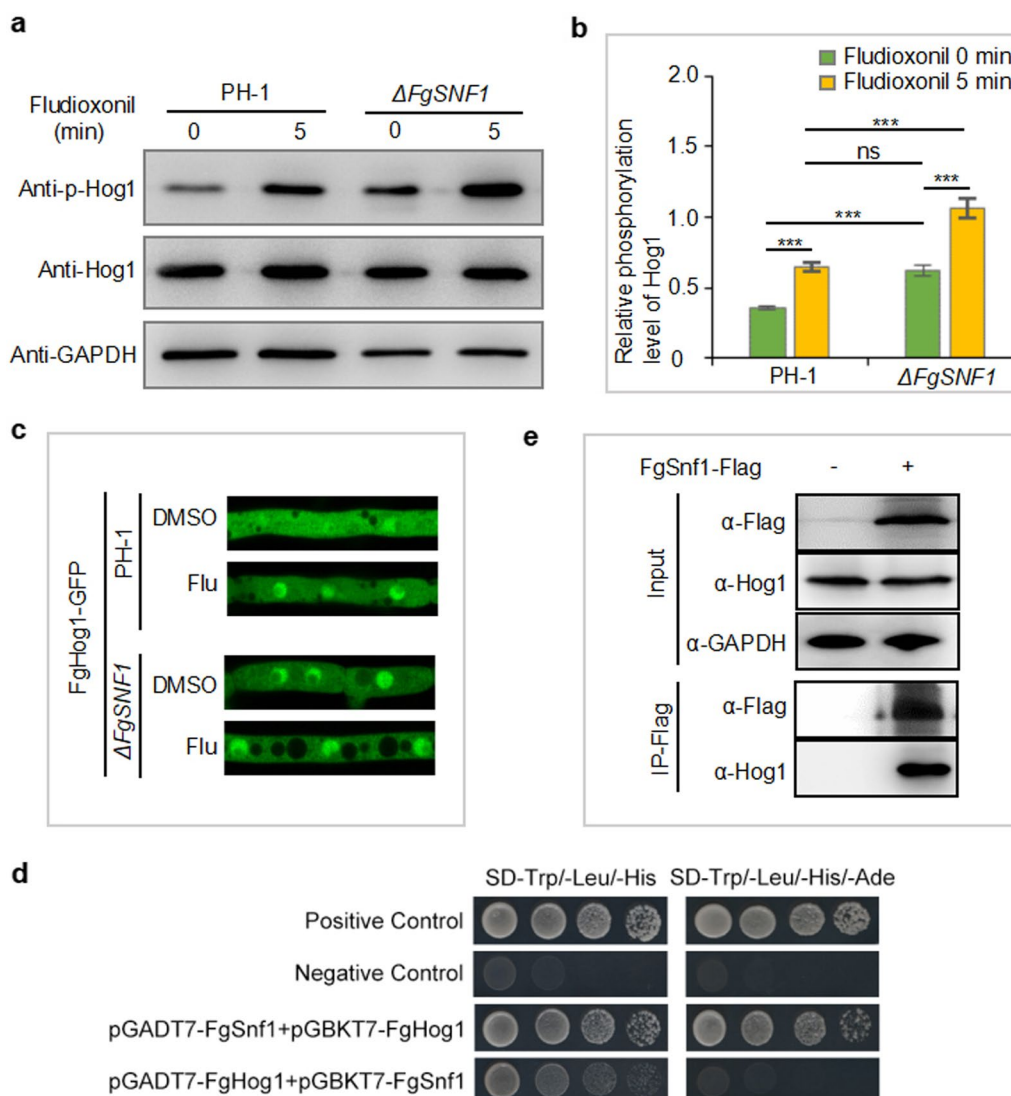
Fig. 5 Protein kinase FgSnf1 interacts with FgHog1 and negatively regulates phosphorylation of FgHog1. **a** The phosphorylation of FgHog1 was detected by immunoblotting in PH-1 and Δ*FgSNF1*, treated with or without fludioxonil. GAPDH was used as a loading control. **b** Quantification of phosphorylation levels of FgHog1 in a. **c** Sub-cellular localization of FgHog1-GFP in PH-1 and Δ*FgSNF1*, strains were treated with fludioxonil at 1 μg/mL or DMSO for 5 min. **d** Interaction between FgSnf1 and FgHog1 was verified by yeast two- hybrid assays. **e** Interaction between FgSnf1 and FgHog1 was verified by Co-IP assays

we detected virulence of these strains on the germ sheath of wheat seedlings. As shown in Fig. 6b, Δ*FgSNF1* and Δ*FgHOG1* caused much less severe symptoms on wheat seedlings than the wild type PH-1. These results indicate that the Snf1-Hog1 pathway was required for the full virulence of *F. graminearum*.

The secondary metabolite DON plays key roles in *F. graminearum* pathogenicity. The formation of toxisomes and accumulation of DON biosynthetic enzyme FgTri1 are markers of DON biosynthesis (Chen et al. 2019). Therefore, we observed toxisomes that were labeled by FgTri1-GFP under a confocal microscope and detected

the accumulation of FgTri1-GFP by immunoblotting in PH-1, Δ*FgSNF1*, and Δ*FgHOG1* strains. As expected, after 48 h of induction in toxin biosynthesis inducing (TBI) medium, typical sub-spheroidal toxisomes were formed surrounding the nucleus in PH-1 hyphae, but no toxisomes were observed in Δ*FgSNF1* or Δ*FgHOG1* (Fig. 6c). Immunoblotting assays further verified that after incubation in TBI for 48 h, the expression of Tri1-GFP protein was induced dramatically in the wild-type PH-1, but not in Δ*FgSNF1* and Δ*FgHOG1*. These results indicate that both Snf1 and the Hog1 pathway are involved in regulating DON biosynthesis.
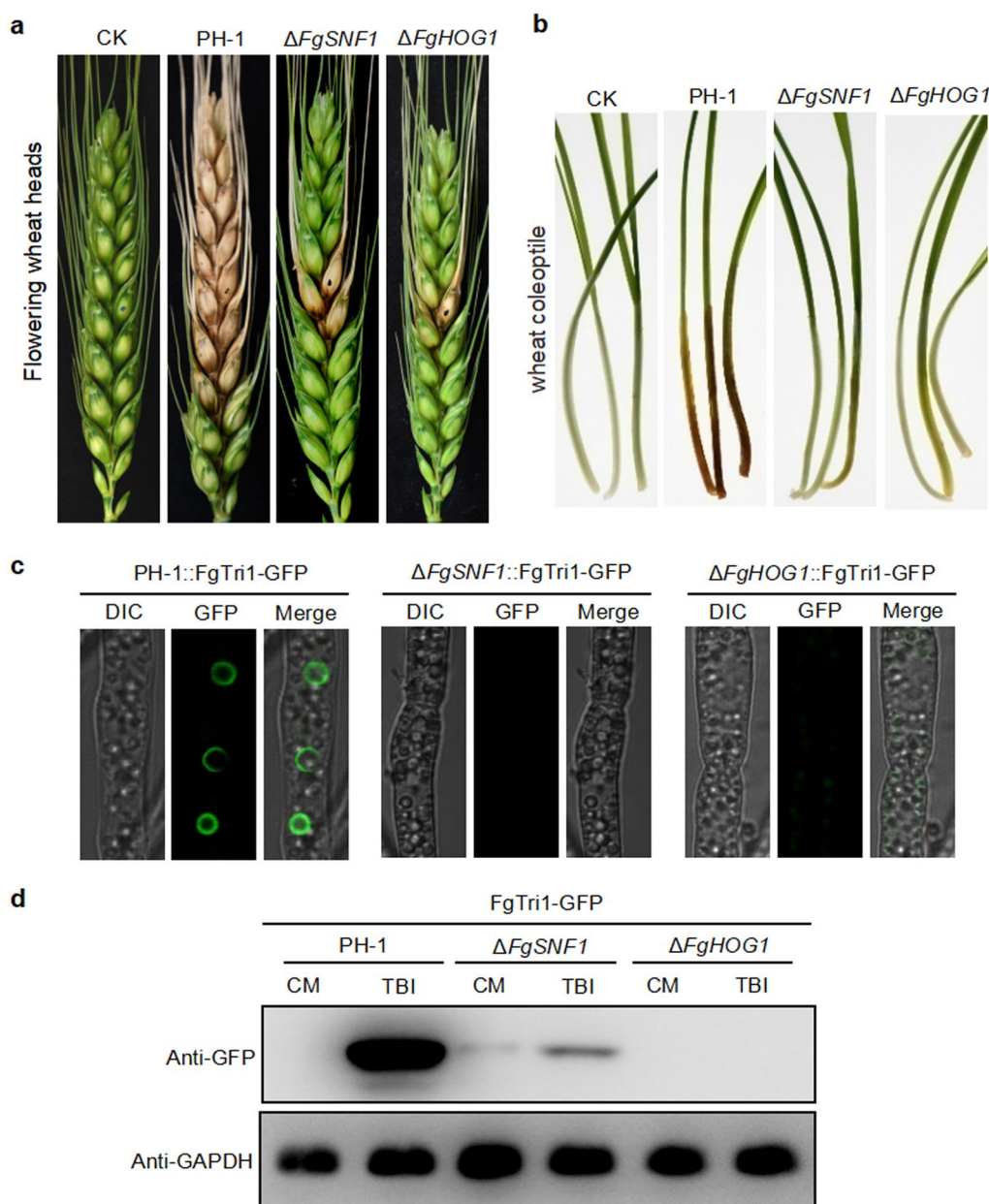
Fig. 6 Protein kinases FgSnf1 and FgHog1 are required for the full virulence and DON biosynthesis in *F. graminearum*. **a** Virulence of each strain on flowering wheat heads. **b** Virulence of each strain on wheat coleoptile. **c** DON toxisome formation of each strain was labelled with FgTri1-GFP. **d** Accumulation of FgTri1-GFP protein in each strain was detected by immunoblotting assays

Discussion

The Hog1 kinase plays a central role in cellular response to external stresses and stimuli in eukaryotes (Brewster and Gustin 2014, Xu et al. 2022). Previous studies showed that HOG MAPK pathway was involved in fludioxonil resistance and deletion or base mutation of these kinases led to fludioxonil resistance (Kojima et al. 2006; Li and Xiao 2008; Wang et al. 2021; Wen et al. 2022). Considering the similar functions of fludioxonil and pyrrolnitrin, it

is conceivable that the mutation of HOG pathway would lead to pyrrolnitrin resistance in fungi. Here, single base mutations were also identified in the HOG MAPK pathway elements (FgOS1, FgOS4, and FgOS5) in pyrrolnitrin-resistant strains of *F. graminearum* (Additional file 2: Table S1). In addition, the base mutations were also identified in the AMP-activated protein kinase FgSnf1 (Additional file 2: Table S1). Deletion of FgSnf1 led to an increased fludioxonil and pyrrolnitrin resistance in *F.*

Wang *et al. Phytopathology Research*   (2023) 5:52

Page 9 of 13

graminearum, although the resistance level of Δ*FgSNF1* was not as high as those of FgHog1 mutants (Fig. 4a, b and Additional file 1: Figure S4a, b), suggesting that the FgSnf1 kinase is involved in fludioxonil response in *F. graminearum*.

The HOG pathway is well characterized in the budding yeast. Hog1 MAP kinase can be activated by either of two branches of upstream osmo-sensing pathways that converge at Pbs2. One involves a two-component histidine kinase phosphorylation system comprised of Sln1, Ypd1, and Ssk1 (Posas et al. 1996), and the other involves a putative membrane protein Sho1, which activates Pbs2 via Ste11 (Maeda et al. 1994; Posas and Saito 1997). In budding yeast, the AMPK Snf1 was reported to negatively regulate activation of Hog1 at different dimensions, including Golgi lipid signaling, ER stress, and metabolic respiration (Piao et al. 2012; Adhikari and Cullen 2014; Mizuno et al. 2015), but the exact mechanisms are unknown. More recently, we found that the calcium-calcineurin pathway transcriptional factor Crz1 regulates activation of Hog1 upon tebuconazole treatment, but not by other stresses, such as osmotic, oxidative, cell wall, and ER stresses in *F. graminearum* (Wang et al. 2023), implying that activation of HOG pathway is affected by different upstream elements under different situations. In this work, we found that FgSnf1 interacted with the FgHog1 directly, and repressed activation and nuclear import of FgHog1, indicating that Snf1 functions as one of the upstream components of Hog1 in *F. graminearum*. This finding is consistent with the observation that Δ*FgHOG1* showed a much higher resistance level to fludioxonil than Δ*FgSNF1*, because FgSnf1 is not the sole upstream regulator for FgHog1.

ER is the largest organelle in cells and is the major site for protein synthesis and folding, lipid and steroid synthesis, carbohydrate metabolism, and calcium storage (Schwarz and Blower 2016; Zeng and Yao 2022). However, the accumulation of misfolded or unfolded proteins in the ER lumen can lead to ER remodeling (Ajoolabady et al. 2022). In budding yeast, Snf1 was reported to negatively regulate the expression of Ssk1 MAPKKK, a core component of HOG pathway, which was induced by the accumulation of unfolded proteins (Mizuno et al. 2015). Since the DON toxisomes were remodeled from ER around nucleus (Chen et al. 2019), our results revealed that DON toxisomes were hardly observed in Δ*FgSNF1* and Δ*FgHOG1*, supporting that Snf1 and the HOG pathway play an important role in regulating ER remodeling in *F. graminearum*.

Previous studies have shown that a large variety of extracellular products could be synthesized by *Burkholderia* species, such as 2-hydroxymethyl-chroman-4-one, altericidins, cepacins, cepaciamides, and phenazines (Parke and Gurian-Sherman 2001; Vial et al. 2007). Although we found that BpW1 was able to produce pyrrolnitrin, and it showed great antagonistic activity towards *F. graminearum*, BpW1 still has comparable inhibitory effect against the fludioxonil-resistant strains PRNJB3-2, Δ*FgSNF1*, and Δ*FgHOG1* (Additional file 1: Figure S5). This result indicates that in addition to pyrrolnitrin, BpW1 may generate different antifungal compounds with different mode of actions as pyrrolnitrin. On the other hand, this result also explained why it was easy to induce pyrrolnitrin- or fludioxonil-resistant strains but we didn't find a strain that is resistant to BpW1. To this point, BpW1 will be helpful for management of fludioxonil resistance in *F. graminearum* in the future.

Conclusions

In this study, we isolated a biocontrol strain BpW1, which produced the antifungal compound pyrrolnitrin and showed great antagonistic activity towards FHB. Genomic resequencing of the pyrrolnitrin-resistant *F. graminearum* strains led to the identification of the single base mutations in the genes encoding the osmoregulation MAP kinase Hog1 and the AMP dependent kinase Snf1. Snf1 was further confirmed to interact with Hog1 and was involved in the response to pyrrolnitrin and its derivate, the fungicide fludioxonil. This study demonstrates that Snf1 interacts with Hog1 to regulate fludioxonil resistance in a pathogenic fungus.

Methods

Biocontrol agents screening

Bacteria were isolated from rhizosphere samples taken from wheat with or without FHB in Hangzhou, China. Each sample was homogenized with a sterilized mortar and pestle. Macerated samples were serially diluted with sterile 0.85% NaCl solution, and the resulting suspensions were plated onto Luria–Bertani (LB) dishes. After 48 h of incubation at 30 °C, colonies were picked randomly based on their morphology, and the picked strains were stored in 20% glycerol at − 70 °C for further investigation.

The antagonistic activities of the collected strains were detected with confrontation. Briefly, bacterial isolates were grown on Waksman's agar (WA, 5 g peptone, 10 g glucose, 3 g beef extract, 5 g NaCl for 1 L, pH 7.2) for 18 h in advance, then the wild type strain (PH-1) of *F. graminearum* were inoculated and co-cultured for 2 days in an incubator at 25 °C. Inhibition zone of each isolate was measured and used for antagonistic activity evaluation. Each isolate was tested in three repetitions, and the experiments were conducted three times independently. To identify the potential bacteria, sequence of 16S ribosomal DNA (rDNA) were amplified with the universal primer pair 27F/1492R (Additional file 2: Table S2) and

Wang *et al. Phytopathology Research* (2023) 5:52

Page 10 of 13

sequenced. The sequences were blasted on the website server (https://blast.ncbi.nlm.nih.gov/Blast.cgi). The phylogenetic analyses with 16S rDNA sequences were conducted in the neighbor-joining method with Mega 5.0.

Characterization of antifungal compounds produced by BpW1

After the BpW1 was inoculated in WA broth for 3 days at 30 °C in a shaker (180 rpm), bacterial cells were removed via centrifugation ($5000 \times g$ for 20 min). The cell-free supernatant was extracted with ethyl acetate for three times, followed by concentrating in a rotary evaporator. After that, the crude ethyl acetate extracts were obtained and dissolved in 1 mL methanol for following experiment. To identify the antifungal compound of *B. pyrrocina* W1, the chromatographic separation was carried through an Agilent Zorbax SB C18 column (150×2.1 mm, 3.5 μm), and the UPLC mobile phases consisted of acetonitrile and water run at a flow rate of 0.3 mL/min. The mass spectrometry assay was performed with an Agilent 6460 triple quadrupole mass spectrometer (Agilent Technologies, USA), equipped with an electrospray ionization (ESI) source. The negative ion scan mode was applied, and the scan range was from 100 m/z to 800 m/z. The Agilent Mass Hunter Workstation was used for data acquisition and processing. Pyrrolnitrin from Xinhong Material Technology co. LTD (Chengdu, China) was used as a standard chemical control.

Fungal strains and culture conditions

The *F. graminearum* PH-1 (NRRL31084) was used as the wild-type strain for generating of gene deletion mutants. Gene deletion mutants were constructed using a PEG-mediated protoplast transformation method (Yu et al. 2014). The potato dextrose agar (PDA) (200 g potato, 10 g D-Glucose, 10 g agar, and 1 L water) was used for fungal growth assays. TBI (30 g sucrose, 1 g KH_2PO_4, 0.5 g $MgSO_4 \cdot 7H_2O$, 0.5 g KCl, 0.01 g $FeSO_4 \cdot 7H_2O$, 1.47 g purtrescine hydrochloride, 200 μL trace element, and 1 L water, pH 4.5) was used for induction of DON production. YEPD (3 g yeast extract, 10 g peptone, 10 g D-Glucose, and 1 L water, pH 6.7) liquid medium was used for preparations of mycelia for confocal and western blotting assays. Conidiation of *F. graminearum* was induced in CMC broth (carboxymethylcelluose sodium 15 g, NH_4NO_3 1 g, yeast extract 1 g, $MgSO_4 \cdot 7H_2O$, 0.5 g, KH_2PO_4, 1 g, and 1 L water) at 25 °C in a shaker (180 rpm) for 6 days.

Determination of BpW1 efficacy against FHB

The control efficacy of BpW1 against FHB was determined in both a growth chamber and in field. Growth chamber assay was conducted according to a previous report with minor modifications (Hu et al. 2014). Briefly, wheat heads of cultivar Jimai 22 (susceptible to FHB) were sprayed with the cell suspension of biocontrol strain BpW1 (1×10^8 CFU/mL) using a hand-held atomizer. The fungicide tebuconazole (2 mg/mL) and sterile water served as the positive and negative controls, respectively. The droplets on wheat heads were air dried for 6 h in a growth chamber and each treated wheat head was sprayed with 3 mL conidial suspension (10^4 conidia/mL of *F. graminearum* strain PH-1 with 0.05% Tween 20). The inoculated wheat heads were kept in the growth chamber at 25 °C and under 95% humidity with a 12 h photoperiod. A total of 25 wheat heads were used for each treatment. After 7 days of incubation, the percentage of infected spikelet in each treatment was examined. The experiment was repeated twice.

Field experiments were performed in Hai'an and Hangzhou in China on wheat cultivars Yangmai 18 (mid-resistant to FHB) and Jimai 22, respectively. The field trials were conducted using a randomized plot design with three replicates for each treatment. Each plot of 10 m² in size was sprayed twice at early and middle-anthesis, respectively, with 2.5 L BpW1 cell suspensions at the concentration of 10^8 CFU/mL amended with 0.05% Tween 20. Fungicide tebuconazole (2 mg/mL) and sterile water served as the positive and negative controls, respectively. After 24 h treatment, each plot was sprayed with 2.5 L conidial suspension (1×10^4 spores/mL) of PH-1. All treatments were performed in the late afternoon before sunset. Twenty-five days after inoculation, FHB disease severity in each plot was recorded. Disease index was assessed with five evaluation classes (0 to 4), which corresponds to a percentage of spikelet showing FHB symptoms (0: 0%, 1: 1 to 25%, 2: 26 to 50%, 3: 51 to 75%, and 4: ≥75%). Disease index (DI) in each plot was calculated using the formula [(Σ number of wheat heads in each class × each evaluation class)/ (total number of wheat heads × 5)] × 100. Efficacy of each treatment was determined by using the formula: [(DI of the negative control-DI of the treatment)/DI of the negative control)] × 100%. The experiment was performed twice and the data was analyzed using Fisher's protected least significant difference test ($P = 0.05$) of SAS (SAS version 8.0; SAS Institute, Cary, NC).

Microscopic observation

For confocal microscopic observation of FgHog1-GFP, the FgHog1-GFP labelled wild type PH-1 and Δ*FgSNF1* were grown in YEPD for 16 h, and then treated with fludioxonil at 0.05 μg/mL for 2 h. DMSO (dimethyl sulfoxide) was used as a dissolvent control for this fungicide. Mycelia of each strain were examined with a Zeiss LSM880 confocal microscope (Gottingen, Niedersachsen,

Wang *et al. Phytopathology Research*   (2023) 5:52

Page 11 of 13

Germany). To determine the toxisomes formation, each gene deletion mutant bearing the FgTri1-GFP was constructed. The resulting strains were incubated in TBI at 28 °C in a shaker (150 rpm) for 48 h, and mycelia of each strain were observed with the confocal microscope described above.

Glycerol quantification

The accumulation of glycerol was quantified with a commercial kit (E1013, Applygen Technologies Inc., Beijing, China). According to the manufacture instructions, each strain was incubated in CM (complete medium) broth for 2 days at 25 °C in a shaker (180 rpm). After treated with fludioxonil at 0.05 μg/mL for 2 h, mycelia of each strain were collected, freeze-dried and ground into powder with liquid nitrogen. Then, 0.2 g of each sample was transferred into a 2 mL centrifuge tube containing 1 mL glycerol isolation buffer. After vortexing for 10 min, the tubes were centrifuged with $10,000 \times g$ for 10 min, and the resulting supernatant was used for glycerol quantification. At the same time, the content of total proteins in each supernatant was determined using a Protein Quantification Kit (P1511, Applygen Technologies Inc., Beijing, China). The glycerol concentrations were calculated as mini-molar per gram protein. Each experiment was repeated three times.

Immunoblotting assay

Fresh mycelia of indicated strains were collected from the corresponding cultures and were frozen in liquid nitrogen for protein extraction. Total proteins were extracted with pre-cold protein lysis buffer (50 mM Tris, 150 mM NaCl, 1 mM EDTA, 1% Triton-100, and 0.1% phenylmethylsulfonyl fluoride) supplemented with 0.1% protein inhibitor cocktail (C60382, Sangon Biotech, Shanghai, China). Total proteins of each sample were dispersed with SDS-PAGE electrophoresis and transferred onto PVDF film. These films were then incubated with the indicated first and second antibodies sequentially. Finally, these blots were imaged by the ImageQuant LAS 4000 mini (GE Healthcare) with an enhanced chemiluminescence (ECL) kit (FD8020, Hangzhou Fude Biological technology co., LTD.). Antibodies used in this work include the anti-hog1 antibody (sc-165978, Santa cruz, CA, USA, 1:2000), anti-phosphorylated-Hog1 antibody (anti-phospho-p38, #9211, Cell Signaling Technology, Boston, MA, USA, 1:2000), anti-GFP antibody (ab31246, Abcam, US, 1:10,000), anti-Flag M2 antibody (F1804, Sigma, USA, 1:5000), anti-GAPDH antibody (EM1101, HuaBio Biotech, Hangzhou, China, 1:10,000), HRP conjugated goat-anti rabbit/ mouse polyclonal IgG antibody (HA1001, HA1006, HuaBio Biotech, Hangzhou, China, 1:5000).

Yeast two hybrid and co-Immunoprecipitation assays

Yeast two hybrid (Y2H) and co-Immunoprecipitation (Co-IP) assays were used to evaluate the interaction between FgSnf1 and FgHog1. For Y2H, sequence of each tested gene was amplified from the cDNA of *F. graminearum* wild-type strain PH-1 with primer pairs indicated in Additional file 2: Table S2. The obtained fragments of FgSnf1 and FgHog1 were constructed into the GAL4-activation domain vector pGADT7 and the yeast GAL4-binding domain vector pGBKT7, respectively (Clontech, MountainView, CA, USA). The pairs of yeast two hybrid plasmids were co-transformed into *S. cerevisiae* strain Y2H Gold. In addition, the pair of plasmids, pGBKT7–53 and pGADT7-T was used as the positive control, while pGBKT7-Lam and pGADT7-T served as the negative control. The resulting transformants were selected on SD-Trp-Leu plates, and then transferred to SD-Trp-Leu-His-Ade medium at 30 °C for 4 days. For Co-IP, Flag-fused Snf1 was transformed into the wild type PH-1. Total proteins were extracted and incubated with Flag-conjugated agarose, and then the input and precipitated samples were analyzed with indicating antibodies by immunoblotting. The original PH-1 strain served as the non-FgSnf1-Flag-labelled control.

Abbreviations

FHB	Fusarium head blight
BCAs	Bio-control agents
SBIs	Sterol biosynthesis inhibitors
HHK	Hybrid histidine kinase
HOG	High-osmolarity glycerol
Drk1	Dimorphism-regulating kinase 1
TPI	Triosephosphate isomerase
MG	Methylglyoxal
Snf1	Sucrose non-fermenting-1
AMPK	AMP-activated protein kinase
TOR	Target of rapamycin
BpW1	*Burkholderia pyrrocina* Strain W1
GFP	Green fluorescence protein
SDS-PAGE	Sodium dodecyl sulfate–polyacrylamide gel electrophoresis
Y2H	Yeast two-hybrid
CO-IP	Co-Immunoprecipitation

Supplementary Information

Additional file 1: Figure S1. BpW1 displays strong antagonistic activity towards a carbendazim-resistant strain isolated from field. The BpW1 was incubated on the plate one day before inoculation of F. graminearum, and then the plates were incubated for 3 days before photography. **Figure S2.** Purification and identification of pyrrolnitrin. **a** The UPLC diagram of BpW1 cell free supernatant. The peak of pyrrolnitrin is marked by arrow at 15.5 min. **b** UPLC analysis of the commercialized standard pyrrolnitrin. **c** The mass spectrogram of commercialized standard pyrrolnitrin. **Figure S3.** The growth and pyrrolnitrin sensitivity of six pyrrolnitrin-resistant strains induced in the lab. The PH-1 strain served as the wild type control. Photos were captured at the 4th day after inoculation. **Figure S4.** Sensitivity of PH-1, ΔFgSNF1, ΔFgHOG1, and PRNJB3-2 strains to pyrrolnitrin. **a** Comparisons in sensitivity of PH-1, ΔFgSNF1, ΔFgHOG1, and PRNJB3-2 on

Wang *et al. Phytopathology Research*   (2023) 5:52

Page 12 of 13

PDA plates supplemented with pyrrolnitrin at different concentrations. **b** Quantification of mycelial inhibition rate. **Figure S5.** BpW1 displays antagonistic activity against the mycelial growth of PH-1, Δ*FgSNF1*, Δ*FgHOG1*, and PRNJB3-2 strains. Photos in upper panel were taken at 3 dpi, and photos of the bottom panel were taken at 10th day of incubation at 25℃ on WA plates.

Additional file 2: Table S1. Bases mutation detected by re-sequencing. **Table S2.** Primers used in this study.

Availability of data and materials
Not applicable.

Declarations

Ethics approval and consent to participate
Not applicable.

Consent for publication
Not applicable.

Competing interests
These authors declare they have no competing interests.

References

Adhikari H, Cullen PJ. Metabolic respiration induces AMPK-and Ire1p-dependent activation of the p38-Type HOG MAPK pathway. PLoS Genet. 2014;10(10): e1004734. https://doi.org/10.1371/journal.pgen.1004734.

Ajoolabady A, Liu S, Klionsky DJ, Lip GYH, Tuomilehto J, Kavalakatt S, et al. ER stress in obesity pathogenesis and management. Trends Pharmaco Sci. 2022;43(2):97–109. https://doi.org/10.1016/j.tips.2021.11.011.

Arima K, Imanaka H, Kousaka M, Fukuda A, Tamura G. Studies on pyrrolnitrin, a new antibiotic I Isolation and properties of pyrrolnitrin. J Antibio, Series a. 1965;18(5):201–4. https://doi.org/10.1254/jjp.15.324.

Brandhorst TT, Kean IRL, Lawry SM, Wiesner DL, Klein BS. Phenylpyrrole fungicides act on triosephosphate isomerase to induce methylglyoxal stress and alter hybrid histidine kinase activity. Sci Rep. 2019;9(1):1–17. https://doi.org/10.1038/s41598-019-41564-9.

Brewster JL, Gustin MC. Hog 1: 20 years of discovery and impact. Sci Signal. 2014;7(343):re7. https://doi.org/10.1126/scisignal.2005458.

Cartwright DK, Chilton WS, Benson DM. Pyrrolnitrin and phenazine production by Pseudomonas cepacia, strain 5 5B, a biocontrol agent of Rhizoctonia solani. Appl Microbiol Bio. 1995;43(2):211–6. https://doi.org/10.1007/BF00172814.

Chen Y, Wang WX, Zhang AF, Gu CY, Zhou MG, Gao TC. Activity of the fungicide JS399–19 against Fusarium head blight of wheat and the risk of resistance. Agr Sci China. 2011;10(12):1906–13. https://doi.org/10.1016/S1671-2927(11)60191-0.

Chen Y, Kistler HC, Ma Z. *Fusarium graminearum* trichothecene mycotoxins: biosynthesis, regulation, and management. Annu Rev Phytopathol. 2019;57(1):15–39. https://doi.org/10.1146/annurev-phyto-082718-100318.

Dean R, Van Kan JAL, Pretorius ZA, Hammond-Kosack KE, Di Pietro A, Spanu PD, Rudd JJ, et al. The Top 10 fungal pathogens in molecular plant pathology. Mol Plant Pathol. 2012;13(4):414–30. https://doi.org/10.1111/j.1364-3703.2011.00783.x.

Hardie DG. AMP-activated/SNF1 protein kinases: conserved guardians of cellular energy. Nat Rev Mol Cell Biol. 2007;8(10):774–85. https://doi.org/10.1038/nrm2249.

Howell CR, Stipanovic RD. Control of *Rhizoctonia solani* on cotton seedlings with *Pseudomonas fluorescens* and with an antibiotic produced by the bacterium. Phytopathology. 1979;69(5):480–2. https://doi.org/10.1094/Phyto-69-480.

Hu W, Gao Q, Hamada MS, Dawood DH, Zheng J, Chen Y, et al. Potential of Pseudomonas chlororaphis subsp. aurantiaca strain Pcho10 as a biocontrol agent against Fusarium graminearum. Phytopathology. 2014;104(12):1289–97. https://doi.org/10.1094/PHYTO-02-14-0049-R.

Jiao Y, Yoshihara T, Ishikuri S, Uchino H, Ichihara A. Structural identification of cepaciamide A, a novel fungitoxic compound from *Pseudomonas cepacia* D-202. Tetrahedron Lett. 1996;37(7):1039–42. https://doi.org/10.1016/0040-4039(95)02342-9.

Kilani J, Fillinger S. Phenylpyrroles: 30 years, two molecules and (nearly) no resistance. Front Microbiol. 2016;7:2014. https://doi.org/10.3389/fmicb.2016.02014.

Kojima K, Bahn Y-S, Heitman J. Calcineurin, Mpk1 and Hog1 MAPK pathways independently control fludioxonil antifungal sensitivity in *Cryptococcus neoformans*. Microbiol-SGM. 2006;152(3):591–604. https://doi.org/10.1099/mic.0.28571-0.

Lawry SM, Tebbets B, Kean I, Stewart D, Hetelle J, Klein BS. Fludioxonil induces Drk1, a fungal group III hybrid histidine kinase, to dephosphorylate its downstream target, Ypd1. Antimicrob Agents CH. 2017;61(2):e01414-e1416. https://doi.org/10.1128/AAC.01414-16.

Lee CH, Kim S, Hyun B, Suh JW, Yon C, Kim C, Lim Y, et al. Cepacidine A, a novel antifungal antibiotic produced by Pseudomonas cepacia. I. Taxonomy, production, isolation and biological activity. J Antibiot. 1994;47(12):1402–5. https://doi.org/10.7164/antibiotics.47.1402.

Lew RR. Turgor and net ion flux responses to activation of the osmotic MAP kinase cascade by fludioxonil in the filamentous fungus *Neurospora crassa*. Fungal Genet Biol. 2010;47(8):721–6. https://doi.org/10.1016/j.fgb.2010.05.007.

Li HX, Xiao CL. Characterization of fludioxonil-resistant and pyrimethanil-resistant phenotypes of *Penicillium expansum* from apple. Phytopathology. 2008;98(4):427–35. https://doi.org/10.1094/PHYTO-98-4-0427.

Maeda T, Wurgler-Murphy SM, Saito H. A two-component system that regulates an osmosensing MAP kinase cascade in yeast. Nature. 1994;369(6477):242–5. https://doi.org/10.1038/369242a0.

Mitchelhill KI, Stapleton D, Gao G, House C, Michell B, Katsis F, et al. Mammalian AMP-activated protein kinase shares structural and functional homology with the catalytic domain of yeast Snf1 protein kinase. J Bio Chem. 1994;269(4):2361–4. https://doi.org/10.1016/S0021-9258(17)41951-X.

Mizuno T, Masuda Y, Irie K. The *Saccharomyces cerevisiae* AMPK, Snf1, negatively regulates the Hog1 MAPK pathway in ER stress response. PLoS Genet. 2015;11(9): e1005491. https://doi.org/10.1371/journal.pgen.1005491.

Moon S-S, Kang PM, Park KS, Kim CH. Plant growth promoting and fungicidal 4-quinolinones from *Pseudomonas cepacia*. Phytochemistry. 1996;42(2):365–8. https://doi.org/10.1016/0031-9422(95)00897-7.

Motoyama T, Kadokura K, Ohira T, Ichiishi A, Fujimura M, Yamaguchi I, et al. A two-component histidine kinase of the rice blast fungus is involved in osmotic stress response and fungicide action. Fungal Genet Biol. 2005;42(3):200–12. https://doi.org/10.1016/j.fgb.2004.11.002.

Parke JL, Gurian-Sherman D. Diversity of the *Burkholderia cepacia* complex and implications for risk assessment of biological control strains. Annu Rev Phytopathol. 2001;39(1):225–58. https://doi.org/10.1146/annurev.phyto.39.1.225.

Parker WL, Rathnum ML, Seiner V, Trejo WH, Principe PA, Sykes R. Cepacin A and cepacin B, two new antibiotics produced by *Pseudomonas cepacia*. J Antibiot. 1984;37(5):431–40. https://doi.org/10.7164/antibiotics.37.431.

Piao H, MacLean Freed J, Mayinger P. Metabolic activation of the HOG MAP kinase pathway by Snf1/AMPK regulates lipid signaling at the Golgi. Traffi. 2012;13(11):1522–31. https://doi.org/10.1111/j.1600-0854.2012.01406.x.

Posas F, Saito H. Osmotic activation of the HOG MAPK pathway via Ste11p MAPKKK: scaffold role of Pbs2p MAPKK. Science. 1997;276(5319):1702–5. https://doi.org/10.1126/science.276.5319.1702.

Posas F, Wurgler-Murphy SM, Maeda T, Witten EA, Thai TC, Saito H. Yeast HOG1 MAP kinase cascade is regulated by a multistep phosphorelay mechanism in the SLN1-YPD1-SSK1 "two-component" osmosensor. Cell. 1996;86(6):865–75. https://doi.org/10.1016/S0092-8674(00)80162-2.

Raymaekers K, Ponet L, Holtappels D, Berckmans B, Cammue BPA. Screening for novel biocontrol agents applicable in plant disease management - A review. Biol Control. 2020;144: 104240. https://doi.org/10.1016/j.biocontrol.2020.104240.

Schwarz DS, Blower MD. The endoplasmic reticulum: structure, function and response to cellular signaling. Cell Mol Life Sci. 2016;73(1):79–94. https://doi.org/10.1007/s00018-015-2052-6.

Shao WY, Zhao YF, Ma ZH. Advances in understanding fungicide resistance in *Botrytis cinerea*. Phytopathology. 2021;111(3):455–63. https://doi.org/10.1094/PHYTO-07-20-0313-IA.

Starkey DE, Ward TJ, Aoki T, Gale LR, Kistler HC, Geiser DM, et al. Global molecular surveillance reveals novel Fusarium head blight species and trichothecene toxin diversity. Fungal Genet Biol. 2007;44(11):1191–204. https://doi.org/10.1016/j.fgb.2007.03.001.

Sun HY, Zhu YF, Liu YY, Deng YY, Li W, Zhang AX, et al. Evaluation of tebuconazole for the management of Fusarium head blight in China. Australas Plant Path. 2014;43(6):631–8. https://doi.org/10.1007/s13313-014-0309-4.

Tang G, Chen Y, Xu J-R, Kistler HC, Ma Z. The fungal myosin I is essential for Fusarium toxisome formation. PLoS Pathog. 2018;14(1): e1006827. https://doi.org/10.1371/journal.ppat.1006827.

Van Bergeijk DA, Terlouw BR, Medema MH, Van Wezel GP. Ecology and genomics of Actinobacteria: new concepts for natural product discovery. Nat Rev Microbiol. 2020;18(10):546–58. https://doi.org/10.1038/s41579-020-0379-y.

Vial L, Groleau M-C, Dekimpe V, Deziel EJJom. *Burkholderia* diversity and versatility: an inventory of the extracellular products. J Microbiol Biotechn. 2007;17(9):1407–29.

Wang W, Fang Y, Imran M, Hu Z, Zhang S, Huang Z, et al. Characterization of the field fludioxonil resistance and its molecular basis in *Botrytis cinerea* from Shanghai Province in China. Microorganisms. 2021;9(2):266. https://doi.org/10.3390/microorganisms9020266.

Wang H, Gai Y, Zhao Y, Wang M, Ma Z. The calcium-calcineurin and high-osmolarity glycerol pathways co-regulate tebuconazole sensitivity and pathogenicity in *Fusarium graminearum*. Pestic Biochem Phy. 2023;190: 105311. https://doi.org/10.1016/j.pestbp.2022.105311.

Wargo MJ, Hogan DA. Fungal-bacterial interactions: a mixed bag of mingling microbes. Curr Opin Microbiol. 2006;9(4):359–64. https://doi.org/10.1016/j.mib.2006.06.001.

Wen Z, Wang J, Jiao C, Shao W, Ma Z. Biological and molecular characterizations of field fludioxonil-resistant isolates of *Fusarium graminearum*. Pestic Biochem Phy. 2022;184: 105101. https://doi.org/10.1016/j.pestbp.2022.105101.

Xu XM, Jeffries P, Pautasso M, Jeger MJ. Combined use of biocontrol agents to manage plant diseases in theory and practice. Phytopathology. 2011;101(9):1024–31. https://doi.org/10.1094/PHYTO-08-10-0216.

Xu M, Wang QH, Wang GH, Zhang X, Liu HQ, Jiang C. Combatting Fusarium head blight: advances in molecular interactions between *Fusarium graminearum* and wheat. Phytopathol Res. 2022;4(1):37. https://doi.org/10.1186/s42483-022-00142-0.

Yu F, Gu Q, Yun Y, Yin Y, Xu JR, Shim WB, et al. The TOR signaling pathway regulates vegetative development and virulence in *Fusarium graminearum*. New Phytol. 2014;203(1):219–32. https://doi.org/10.1111/nph.12776.

Zeng HY, Yao N. Sphingolipids in Plant Immunity. Phytopathol Res. 2022;4(1):20. https://doi.org/10.1186/s42483-022-00125-1.

Zheng D, Zhang S, Zhou X, Wang C, Xiang P, Zheng Q, et al. The FgHOG1 pathway regulates hyphal growth, stress responses, and plant infection in *Fusarium graminearum*. PLoS ONE. 2012;7(11): e49495. https://doi.org/10.1371/journal.pone.0049495.

Zhou F, Hu HY, Song YL, Gao YQ, Liu QL, Song PW, et al. Biological characteristics and molecular mechanism of fludioxonil resistance in *Botrytis cinerea* from Henan province of China. Plant Dis. 2020;104(4):1041–7. https://doi.org/10.1094/PDIS-08-19-1722-RE.